



Effects of specimen size on linear energy storage and dissipation laws of red sandstone under uniaxial compression

Fengqiang Gong^{1,2,3} · Yuxin Ni² · Hangyu Jia³

Received: 20 January 2022 / Accepted: 10 August 2022 / Published online: 26 August 2022
© Springer-Verlag GmbH Germany, part of Springer Nature 2022

Abstract

Size effect is a project that cannot be ignored in rock mechanics. To investigate the size effect on the energy distribution and evolution laws, several groups of uniaxial compression tests and single-cycle loading–unloading uniaxial compression tests were performed on red sandstone specimens of different sizes (diameters of 25, 37, 50, 75, and 100 mm; a constant length-to-diameter ratio of 2.0) using the INSTRON 1346 test system. Experimental results show that mechanical properties are influenced by specimen size while failure mode has no significant variation for different diameter specimens. Strain energy parameters (input strain energy, elastic strain energy, and dissipated strain energy) under each unloading stress level were calculated by integration based on the stress–strain curves. The input strain energy, elastic strain energy, and dissipated strain energy nonlinearly increase with actual unloading stress levels, expressed as unified quadratic function relationships. Furthermore, the elastic strain energy and dissipated strain energy have linear relationships with the input strain energy. Through analyzing coefficients of variation of common parameters, it was found that the energy storage capacity of rock was not sensitive to the specimen size, and therefore, the energy storage coefficient could be considered an essential property of rock materials.

Keywords Size effect · Linear energy storage law · Linear energy dissipation law · Energy evolution characteristics · Uniaxial compression test · Red sandstone

List of symbols

E_i	Input strain energy
E_d	Dissipated strain energy
E_e	Elastic strain energy
σ_c	Peak strength
σ_{cn}	Normalized strength of specimens
σ_c^D	Peak strength of “D” diameter specimens
k	Preset unloading stress level
i	Actual unloading stress level
σ_c^k	Peak strength of specimens with preset unloading stress level k
$k\sigma_c$	Preset unloading stress

E_i^i	Input strain energy at actual unloading stress level i
E_e^i	Elastic strain energy at actual unloading stress level i
E_d^i	Dissipated strain energy at actual unloading stress level i
E_i^D	Input strain energy of “D” diameter specimens
E_e^D	Elastic strain energy of “D” diameter specimens
E_d^D	Dissipated strain energy of “D” diameter specimens
ϵ_0	Permanent strain after unloading
ϵ_u	Strain at unloading point
ϵ_p	Peak strain
D	Specimen diameter
L/D	Ratio of specimen length to the specimen diameter
CoV	Coefficient of variation
β	Standard deviation
μ	Average value

✉ Fengqiang Gong
fengqiangg@126.com

¹ Engineering Research Center of Safety and Protection of Explosion & Impact of Ministry of Education (ERCSPPEIME), Southeast University, Nanjing 211189, China

² Southeast University-Monash University Joint Graduate School, Southeast University, Suzhou 215123, China

³ School of Resources and Safety Engineering, Central South University, Changsha 410083, China

Abbreviations

ISE	Input strain energy
ESE	Elastic strain energy
DSE	Dissipated strain energy

LES	Linear energy storage
LED	Linear energy dissipation
UC	Uniaxial compression
SCLUC	Single-cycle loading–unloading uniaxial compression
ESC	Compression energy storage coefficient
EDC	Compression energy dissipation coefficient

Introduction

Owing to the complex formation conditions and long-term geological tectonics, rocks often contain various types of microscopic cracks, which directly affect their mechanical properties (Perie and Monteiro 1991; Liu et al. 1998). In rock mechanics, the specimen size is a negligible factor which may influence micro-defects and the corresponding mechanical properties. Meanwhile, rock deformation and failure are state instability phenomenon driven by energy, whose essential characteristic is energy transformation (Xie et al. 2005; Li and Cai 2021; Su et al. 2021). Thus, it is significant to investigate the size effect of rocks from an energy point of view.

Many experimental studies and numerical simulations have been carried out to investigate the size effect on mechanical properties. The peak compressive strength decreases with L/D regardless of material types (John 1972; Hawkins 1998; You and Zou 2000; Lei et al. 2019), loading rates (Liang et al. 2013; Meng et al. 2016), and temperature (Su et al. 2015). Meanwhile, several models which reflect relationship between the peak strength and diameters were proposed, such as an exponential function suggested by Liu et al. (1998), the H-B model (Hoek and Brown 1980), and MFSL model (Carpinteri et al. 1995). Many experimental data were used for validating and modifying these models by later researchers (Hawkins 1998; Pells 2004; Darlington et al. 2011; Masoumi et al. 2016; Darbor et al. 2019; Rong et al. 2018). When the length-to-diameter ratio (L/D) varies from 1 to 3, Thuro et al. (2001) pointed out that the size effect on rock damage and elastic modulus is quite remarkable. Under uniaxial compression (UC) and uniaxial cyclical compression tests, Guo et al. (2017) noted that AE counts and AE energy decrease with an increase in the L/D ratio. Walton (2018) pointed out that crack initiation and damage stresses are not related to specimen sizes. Wu et al. (2021) conducted UC tests on specimens with a small size ($D = 20\sim 50$ mm) and analyzed the reason for size effects through CT scanner and 3D profilometer. Li et al. (2021) modified the universal equation derived from Song et al. (2018) to describe the relationship among the peak strength, specimen size, and loading direction. Kasyap and Senetakis (2022) observed small-scale size effects through various parameters (displacements at peak stress, tangential stiffness, and shear band formations) from shearing tests.

In addition to mechanical properties of rocks, energy is also an important topic on which researchers focus. Gong et al. (2018, 2019) found that the elastic strain energy (ESE) and dissipation strain energy (DSE) linearly increase with the input strain energy (ISE), which are named linear energy storage (LES) law and linear energy dissipation (LED) law, respectively. Khoramishad et al. (2014) studied size effects on the fracture energy of rocks and modified Bazant's (1984) size effect law based on the fracture process zone. Meng et al. (2016) and Liang et al. (2016) pointed out that strain energy parameters (ISE, ESE, and DSE) decrease with L/D regardless of strain rates and described relationships between strain energy parameters and L/D with a power function (Meng et al. 2016) and a logarithmic regression function (Liang et al. 2016). In unloading rockburst tests, Zhao and He (2017) pointed out that fragment kinetic energy is not sensitive to sample size when the height-to-thickness ratio is less than 3. Zhao et al. (2022) discussed the energy storage limit and failure mode of sandstone under different L/D . Kasyap et al. (2022) analyzed relationships between the energy loss and fracture width and studied the total kinetic energy under different fracture distances.

Most investigations concentrated on the size effect from the aspect of mechanical properties, but the size effect on rock energy characteristics has less well been investigated. Furthermore, present research mostly focused on the relationship between strain energy parameters and L/D , but rarely investigated the internal relationships among strain energy parameters under different specimen sizes. In addition, it is generally known that energy storage and dissipation are inevitable in the process of rock damage and failure. Gong et al. (2018) defined the energy storage coefficient (ESC) and energy dissipation coefficient (EDC), among them, ESC can reflect the storage capacity of ESE during loading. The ESE at the peak strength can be accurately obtained through ESC, thus improving a series of rockburst proneness criteria (Gong et al. 2020, 2021a, 2022). EDC can be widely used in proposing a new damage variable and establishing a damage constitutive model based on energy dissipation (Gong et al. 2021b). Therefore, investigating internal relationships among strain energy parameters under different specimen sizes and studying the size effect on ESC and EDC is of great significance.

In this study, five groups of single-cycle loading–unloading uniaxial compression (SCLUC) tests were performed on red sandstone using an INSTRON 1346 testing system. The rock specimens had the constant $L/D = 2/1$ and five contrasting diameters: 25, 37, 50, 75, and 100 mm. Based on test results, relationships among ISE, ESE, and DSE under different specimen sizes were clearly presented, and size effects on ESC and EDC were analyzed. This study would extend the applicable scope of LES and LED laws and enrich energy-based research on rock materials.

Experimental methodology

Specimen preparation

Rock specimens used in this study was red sandstone collected from Wuding County, Yunnan Province, China. The rock cores were first sampled from the same intact rock block, which had a uniform texture. Then, these cores were processed into cylindrical specimens. The L/D of the prepared specimens was 2, and the specimen diameters were 25, 37, 50, 75, and 100 mm, respectively (see Fig. 1). The prepared specimens had integrated and compact textures, and there were no visible cracks on their surfaces. The average density and P-wave velocity of the rock specimens were 2450 kg/m^3 and 3411 m/s , respectively. Specific data are presented in Table 1. The specimen identification (ID) was organized in the form of “C-D-b,” wherein “C” means the compression test, “a” means the specimen diameter (mm), and “b” denotes the serial number of specimens in the “D” diameter group. Noteworthy, “b = 0” represents that the specimens are used to perform UC tests while “b = 1~6” on behalf of SCLUC tests with various unloading stress levels.

Test equipment

An electro-hydraulic servo-controlled testing system (INSTRON 1346) shown in Fig. 2 was used for the experiment. This test system comprises a control and data collection system, a loading system, a hydraulic transmission system, and a 2.5-mm-displacement extensometer. During the compression tests, the maximum axial loading force is 2000 kN. The strain and stress were obtained through a displacement extensometer and a hydraulic transmission system. An

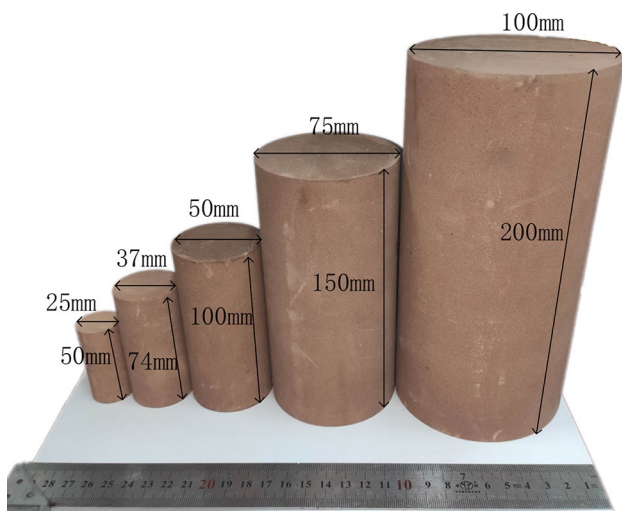


Fig. 1 Photograph of the typical prepared specimens of different sizes

extensometer was used to measure the axial deformation of specimens. It was noted that two rigid blocks were placed between the specimen and equipment indenters to reduce the end friction effect. For the purpose of obtaining actual axial deformations of specimens, the axial deformation of these two rigid blocks was deducted.

Test process

A monotonic UC test and five to six SCLUC tests were performed on specimens of each size group to investigate the size effect of red sandstone. For the monotonic UC test, one to three rock specimens were tested with a monotonically increasing loading until failure to obtain the (average) peak strength σ_c . For SCLUC tests, according to the obtained σ_c , five unloading stresses were preset as $k\sigma_c$ (where the preset unloading stress level $k = 0.1, 0.3, 0.5, 0.7, \text{ and } 0.9$). In SCLUC tests, the specimen was first loaded, then unloaded once it reached the preset unloading stress, and a second loading was applied until it failed. The loading path of the SCLUC test is shown in Fig. 3.

The monotonic UC test and SCLUC tests were performed for specimens in each size group. Notably, the actual unloading stress level i is the ratio of the unloading stress to the actual peak strength under SCLUC tests ($i = k\sigma_c/\sigma_c^k$). The loading rate of the monotonic UC test was 1 MPa/s ; for SCLUC tests, in order to prevent specimens from sudden failure near the peak point, a force-controlled and then displacement-controlled loading mode was used. In specific, the loading rate of the initial loading and unloading processes was 1 MPa/s , and the loading rate of the second loading process was 1 MPa/s before $0.8\sigma_c$, then 0.001 mm/s until failure.

Energy calculation method

According to the thermodynamics law, the relationship between ISE, ESE, and DSE is as follows (Kidybinski 1981):

$$E_i^i = E_c^i + E_d^i \tag{1}$$

where i is the actual unloading stress level ($0 \leq i \leq 1$), E_i^i , E_c^i , and E_d^i are the ISE, ESE, and DSE at the actual unloading stress level i , respectively.

According to the schematic diagram shown in Fig. 4, strain energy parameters at the unloading point could be determined. ISE is the total input strain energy resulting from the work done by external forces and ISE is equal to the area between the initial loading curve and the horizontal axis (Eq. (2)). ESE could be determined as the area between the unloading curve and the horizontal axis (Eq. (3)). DSE equals ISE minus ESE (Eq. (4)). The specific equations are shown as follows:

Table 1 Basic parameters of specimens

Sp. ID	Diameter (mm)	Height (mm)	Mass (g)	Density (kg/m ³)	P-wave velocity (m/s)	Peak strength σ_c (MPa)	Peak strain ϵ_p	Elastic modulus (GPa)
C-25-0	24.24	50.30	57	2456.81	3153	72.91	0.0092	10.28
C-25-1	24.20	50.30	55	2378.45	3153	73.86	0.0092	9.91
C-25-2	24.17	50.39	56	2423.38	3159	67.89	0.0090	9.33
C-25-3	24.34	50.30	57	2436.67	3183	74.03	0.0093	10.28
C-25-4	24.16	50.33	56	2428.27	3155	73.52	0.0098	9.13
C-25-5	24.23	50.33	57	2457.38	3175	73.76	0.0092	9.77
C-37-0	36.30	74.15	182	2372.89	3162	66.05	0.0075	11.68
C-37-1	36.30	74.28	184	2394.77	3201	69.24	0.0084	11.31
C-37-2	36.30	74.28	184	2394.77	3194	69.39	0.0078	11.75
C-37-3	36.30	74.18	183	2384.96	3129	64.94	0.0082	11.11
C-37-4	36.30	74.12	182	2373.85	3187	62.57	0.0074	11.21
C-37-5	36.30	74.27	184	2472.16	3157	69.59	0.0083	11.63
C-37-6	36.30	74.25	184	2395.73	3186	68.38	0.0085	11.61
C-50-0	49.36	100.46	456	2373.29	3067	50.88	0.0074	9.34
C-50-1	48.94	100.49	464	2455.83	3092	68.97	0.0075	12.72
C-50-2	48.98	100.60	464	2466.41	3173	72.53	0.0074	13.14
C-50-3	48.73	100.25	463	2477.62	3213	71.02	0.0081	12.51
C-50-4	48.97	100.75	465	2451.76	3085	73.34	0.0081	12.46
C-50-5	48.75	100.22	458	2472.16	3156	70.02	0.0086	11.95
C-50-6	48.73	100.43	463	2473.18	3415	63.39	0.0069	13.01
C-75-0	74.45	150.40	1639	2504.56	3169	78.46	0.0088	12.51
C-75-1	75.10	150.30	1644	2470.55	3218	77.92	0.0083	12.70
C-75-2	75.16	150.05	1644	2470.71	3199	78.11	0.0086	12.66
C-75-3	75.01	150.08	1639	2472.57	3203	78.75	0.0084	12.68
C-75-4	75.14	150.10	1638	2462.19	3193	76.29	0.0086	12.32
C-75-5	75.12	149.90	1641	2471.30	3209	76.81	0.0084	12.70
C-100-0	100.02	199.95	3837	2443.58	3349	77.05	0.0080	12.77
C-100-1	99.85	200.54	3837	2444.70	3393	80.87	0.0080	14.06
C-100-2	99.05	199.65	3836	2494.77	3386	81.96	0.0084	13.61
C-100-3	100.65	199.75	3846	2421.17	3365	76.85	0.0083	12.71
C-100-4	99.65	199.95	3843	2465.61	3346	79.12	0.0082	13.06
C-100-5	99.95	199.95	3835	2445.73	3383	79.47	0.0079	13.94

$$E_i^i = \int_0^{\epsilon_u} f(\epsilon) d\epsilon \quad (2)$$

is the permanent strain after unloading, and ϵ_u is the strain at the unloading point.

$$E_c^i = \int_{\epsilon_0}^{\epsilon_u} f_u(\epsilon) d\epsilon \quad (3)$$

Results

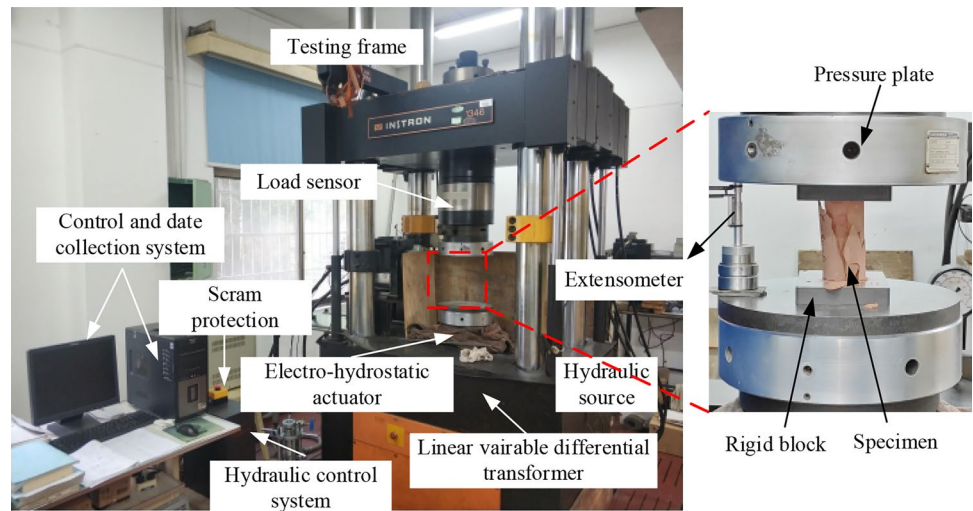
Mechanical properties of red sandstone with different sizes

$$E_d^i = E_i^i - E_c^i = \int_0^{\epsilon_u} f(\epsilon) d\epsilon - \int_{\epsilon_0}^{\epsilon_u} f_u(\epsilon) d\epsilon \quad (4)$$

where $f(\epsilon)$ and $f_u(\epsilon)$ are the curvilinear functions of initial loading process and the unloading process, respectively. ϵ_0

Stress–strain curves of red sandstone specimens of different sizes are shown in Fig. 5. The concavity of stress–strain curves slightly decreased with the specimen

Fig. 2 INSTRON 1346 test system



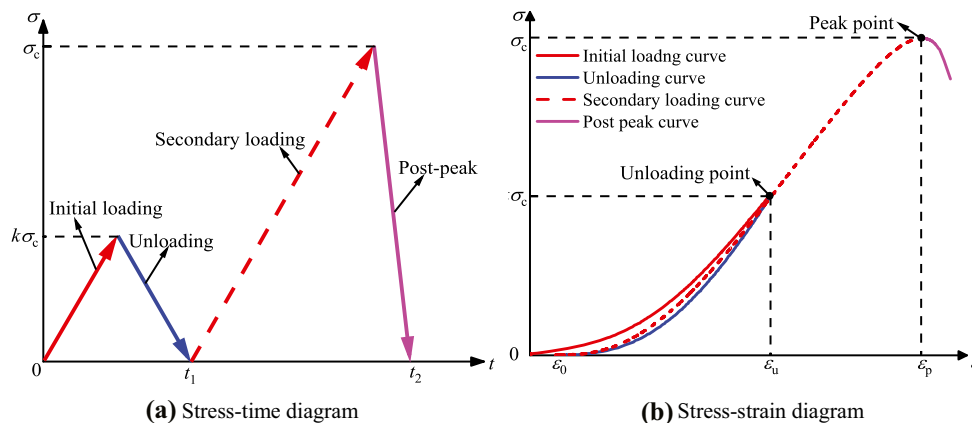
size; thus, the elastic modulus increased. Stress–strain curves dropped steeply when reaching the peak point regardless of specimen sizes, exhibiting brittle failure characteristic. Specimens of $D = 25$ mm showed the largest peak strain, and the peak strain varied slightly for specimens from $D = 37$ to $D = 100$ mm. When the diameter of specimens changed from 37 to 100 mm, the peak compression strength increased slightly. For specimens with a diameter of 25 mm, the peak compression strength was at a medium level.

From stress–strain curves of SCLUC tests shown in Fig. 5b~f, it was observed that the secondary loading curve passed the unloading point. This finding confirms that the single-cycle loading and unloading processes have no effect on its full UC process. In addition, the unloading curves no longer returned to the coordinate origin (0,0), indicating that there was a permanent plastic strain after unloading and energy dissipation existed during the loading and unloading process.

Failure characteristics of red sandstone with different sizes

Figure 6 shows pictures of specimens after failure. The failure mode of red sandstone was axial splitting failure regardless of specimen sizes. In Fig. 6a and c, there was one main crack approximately along the loading direction and several small cracks appeared near the main crack. In Fig. 6b, numerous axial cracks along the loading direction appeared in the outer surface of the rock specimen, exhibiting obvious splitting failure characteristics. Figure 6d and e exhibited multiple failure surfaces and rock fragments were mostly in block and flake forms. As specimen sizes increased, the number of rock fragments increased. For specimens of small diameters in Fig. 6a~c, only a small number of rock fragments fell inside the equipment pressure head. While for specimens of larger diameters in Fig. 6d and e, lots of fragments dropped from the rock parent body and fell outside the equipment indenter. The remaining rock specimen body

Fig. 3 Load path of the SCLUC test: **a** stress–time diagram, and **b** stress–strain diagram



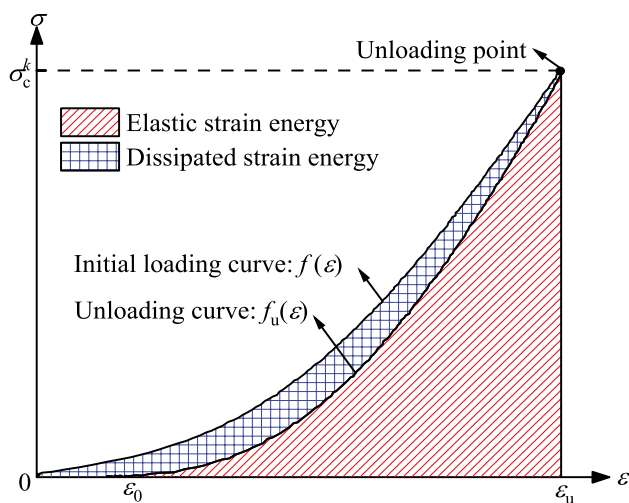


Fig. 4 Schematic of the energy calculation method at the actual unloading stress level

after failure were in the form of two cones. Conical failure shown in Fig. 6d and e was caused by the “end friction effect” that the friction between specimen ends and loading plates limited the radial deformation at both specimen ends (Wu 2021).

Gong et al. (2018) defined the far-field ejection mass ratio as a semi-quantitative indicator to evaluate rockburst proneness. However, the far-field and near-field were defined according to standard specimens ($D \times L = 50 \text{ mm} \times 100 \text{ mm}$). Whether this indicator could be used for non-standard specimens needed further research, because the range of near-field would increase with the specimen diameter. Herein, based on the experimental data and failure characteristics of standard specimens, red sandstone had a far-field ejection mass ratio of 0.13 that a small number of blocks were ejected and mostly fell within the equipment indenter. Additionally, through applying rockburst proneness criteria suggested in Gong et al. (2018) for quantitative analysis, the residual elastic energy was 97.4 kJ/m^3 . These results indicate that red sandstone had a low rockburst proneness.

Energy evolution characteristics of red sandstone with different sizes

Invoking the energy calculation method in the “Energy calculation method” section, the ISE, ESE, and DSE at different i were achieved. When analyzing the energy evolution characteristics of red sandstone with i , a coordinate origin (0,0) was added to represent the initial state where all strain energy parameters could be zero. The ISE, ESE, and DSE of specimens with different sizes under different unloading stress levels were shown in Fig. 7. The ISE, ESE, and

DSE all nonlinearly increased with the i regardless of specimen sizes. Relationships between E_i^i , E_e^i , E_d^i and i were fitted with quadratic functions. Specific fitting equations and their coefficients of determination (R^2) were also expressed in Fig. 7. It was found that there were uniform nonlinear relationships between E_i^i , E_e^i , E_d^i and i in the range of $D = 25 \sim 100 \text{ mm}$ with the R^2 of 0.9674, 0.9657, and 0.9620, respectively. These high R^2 values showed that specimen size did not have significant impacts on the variation rate of strain energy parameters with i . During the deformation and failure process of rock, the ISE converted into the ESE and DSE. Additionally, the ISE has the fastest increasing rate while DSE has the slowest one with i . The specimen size would not change this energy conversion mechanism that ESE was always larger than DSE, indicating that most of the ISE was stored as the ESE and a limited portion was dissipated. Through these relationships, strain energy parameters at any unloading stress levels with any specimen sizes could be obtained.

Linear energy storage and dissipation laws of red sandstone with different sizes

For specimens with five different diameters, relationships between the ISE and ESE, DSE were shown in Fig. 8. During data fitting, the point (0, 0) was artificially added for the correction deviation; this coordinate origin corresponds to the ideal situation in which both the ESE and DSE are 0 when the ISE is 0. Figure 8 shows that ISE has good linear correlations with both ESE and DSE regardless of specimen sizes, which could be described as the LES law and LED law, respectively. The LES and LED laws under different specimen sizes could be expressed as followed:

$$E_e^D = aE_i^D + b \quad (5)$$

$$E_d^D = (1 - a)E_i^D - b = cE_i^D - b \quad (6)$$

where E_i^D , E_e^D , and E_d^D are ISE, ESE, and DSE of specimens of diameter D (mm), respectively, and a and b are fitting parameters. “ a ” and “ c ” can be defined as compression energy storage coefficient (ESC) and compression energy dissipation coefficient (EDC), respectively.

For specimens with $D = 25, 37, 50, 75, \text{ and } 100 \text{ mm}$, R^2 of linear fitting functions between the ISE and ESE were 0.9998, 0.9991, 0.9979, 0.9985, and 0.9998, respectively, whereas R^2 of the fitting functions between the ISE and DSE were 0.9993, 0.9967, 0.9934, 0.9957, and 0.9998, respectively. High fitting levels demonstrate that the LES and LED laws exist for specimens of any size, further extending the application scope of linear laws.

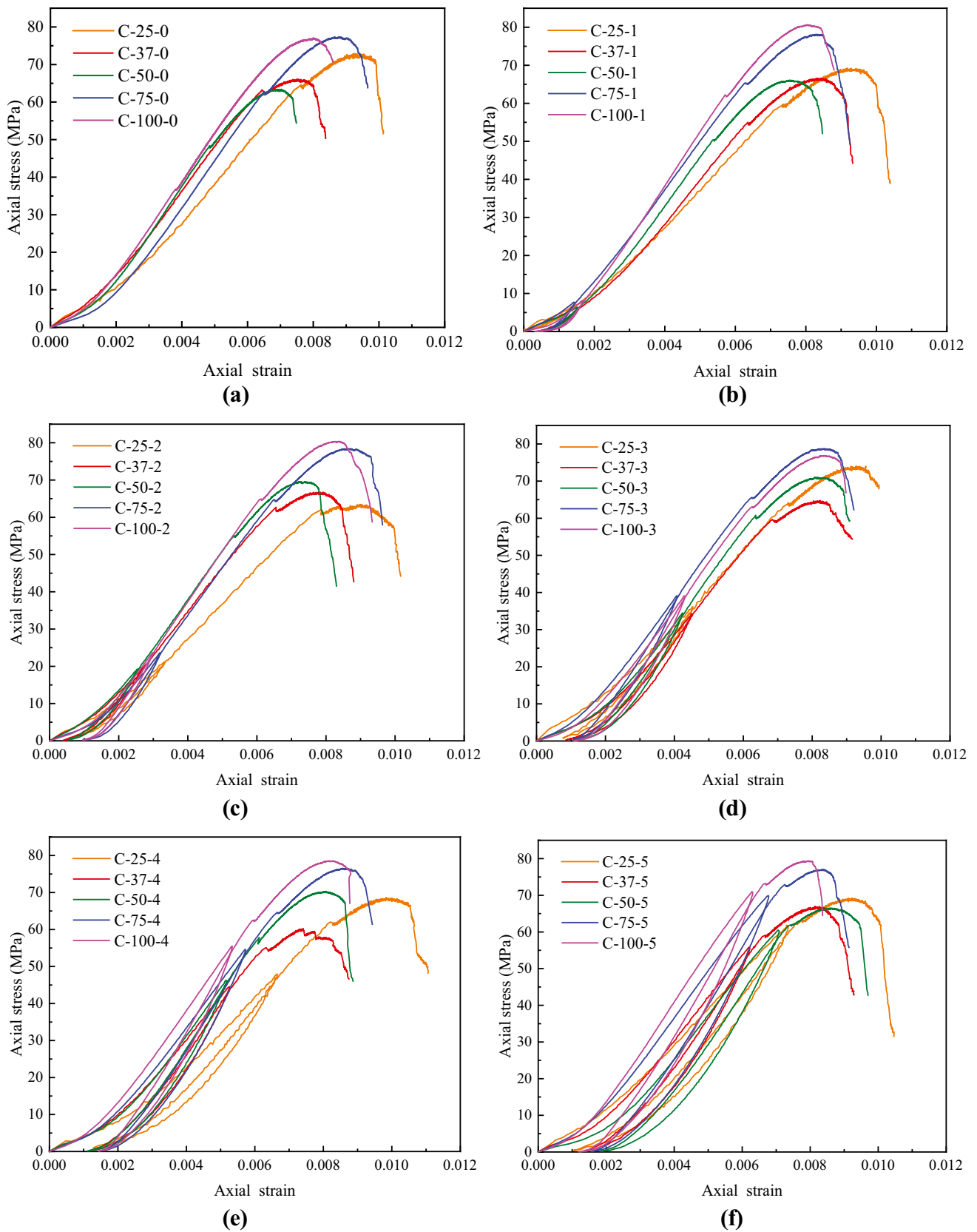
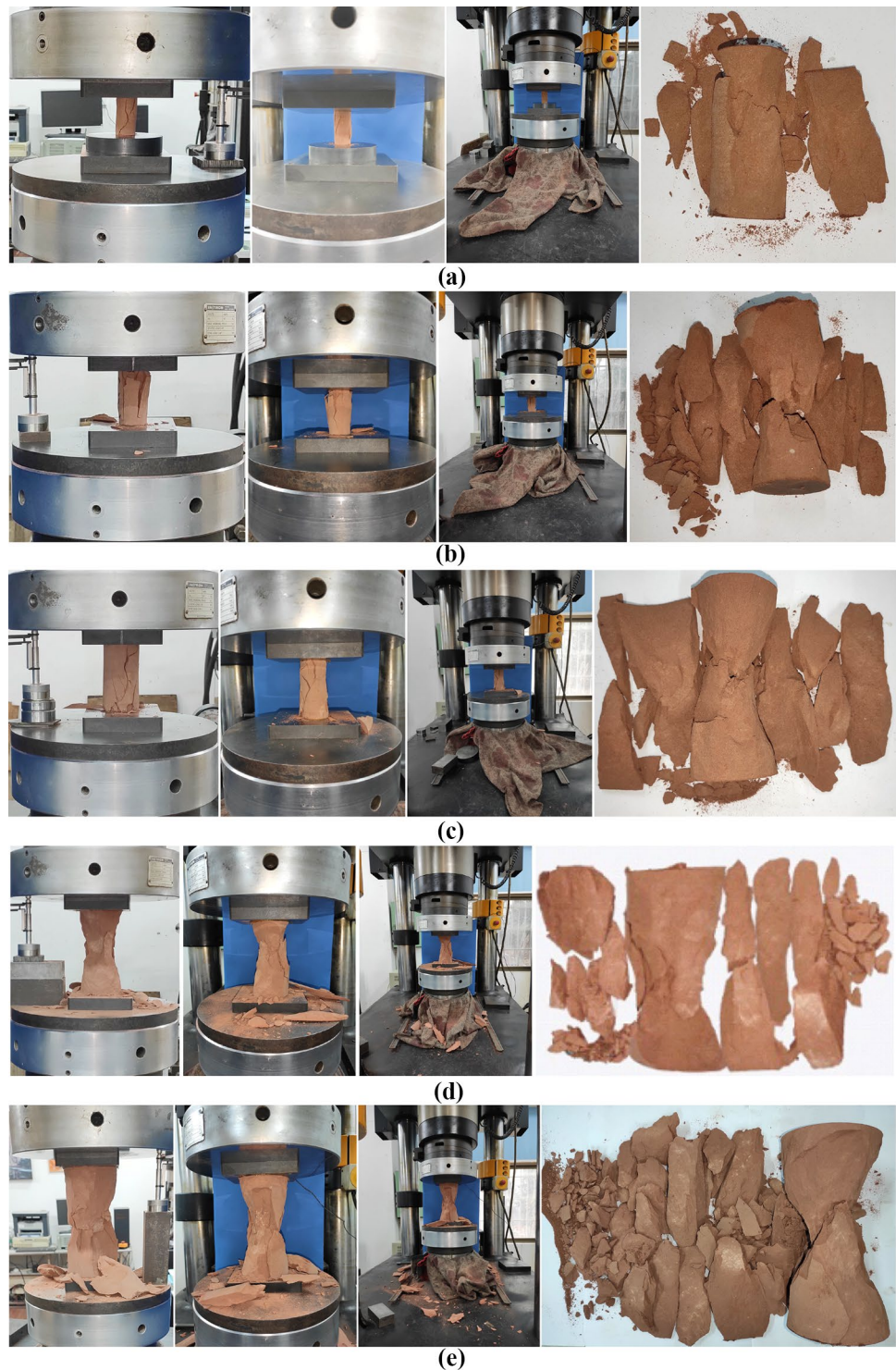


Fig. 5 Stress–strain curves of specimens of different sizes under different unloading stress level: **a** $k = 0$, **b** $k = 0.1$, **c** $k = 0.3$, **d** $k = 0.5$, **e** $k = 0.7$, and **f** $k = 0.9$

Fig. 6 Failure characteristics of specimens with different sizes: **a** C-25-4, **b** C-37-1, **c** C-50-5, **d** C-75-2, and **e** C-100-2



Through comparing *a*, *b*, and *c*, it was observed that *b* was much smaller than *a* and *c*. Therefore, when discussing size effect on linear energy storage and dissipation laws, the intercept *b* could be ignored. Thus, the size effect on the LES and LED laws could be evaluated through researching the ESC and EDC of specimens of different sizes. For specimens of five various diameters, values of ESC were 0.6688,

0.6487, 0.6439, 0.6306, and 0.6505, respectively, whereas values of EDC were 0.3312, 0.3513, 0.3561, 0.3694, and 0.3494, respectively (see Fig. 9). The difference between the maximum ESC (or EDC) and minimum ESC (or EDC) was only 0.0382, indicating that ESC and EDC changed slightly with the variation of specimen diameters. Consequently, unified LES and LED laws can be proposed for specimens of

$D = 25\text{--}100$ mm (Fig. 10) whose R^2 are 0.9981 and 0.9936, respectively. ESC and EDC of unified linear laws were 0.6488 and 0.3512, respectively. Based on the unified LES and LED laws, as long as the ISE was calculated through integration, accurate ESE and DSE of specimens of any diameters could be obtained.

Discussion

Size effect on peak strength of specimens with L/D of 2

To investigate the size effect on the peak strength for specimens whose L/D is 2, results in this study and previous research were analyzed. Table 2 summarized conclusions

about the size effect on the uniaxial compressive strength in reported literature. Conclusions resulted from different literature were different. From the point of view of statistical distribution, rock specimens contained micro-defects of different scales, and rock specimens with larger size were possible to contain more micro-defect, thus leading to lower strength (Çelik 2017). In addition, friction force existed between the rigid block and end faces more or less, resulting in a lateral binding force near the end face. Therefore, the peak compressive strength of rocks was negatively correlated with length and positively correlated with diameter. The size effect of rock materials on the peak strength was caused by a combination of several factors (Yang et al. 2005), and thus conclusions obtained from different studies might vary.

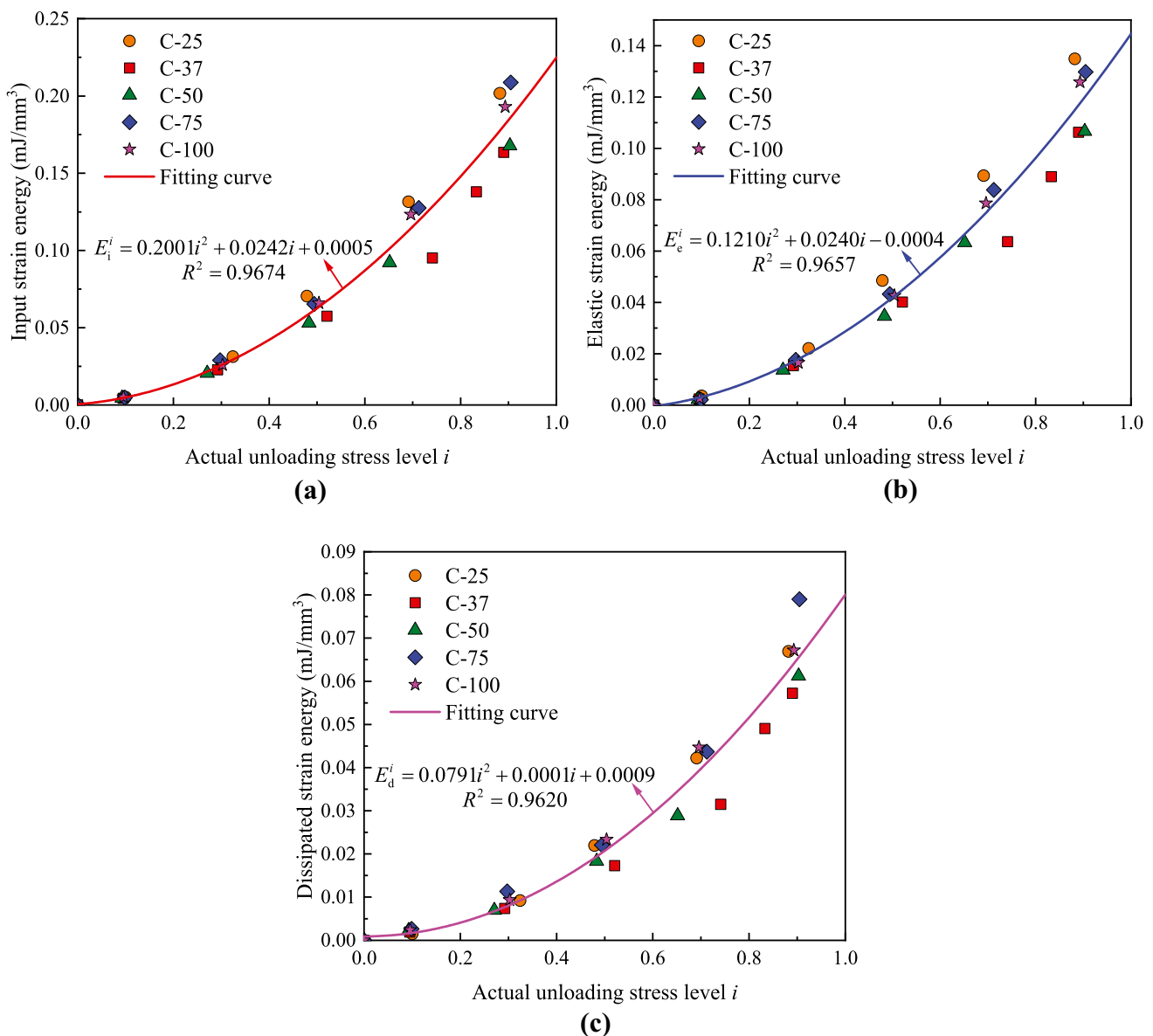


Fig. 7 Relationships between the actual unloading stress level i and **a** ISE, **b** ESE, and **c** DSE

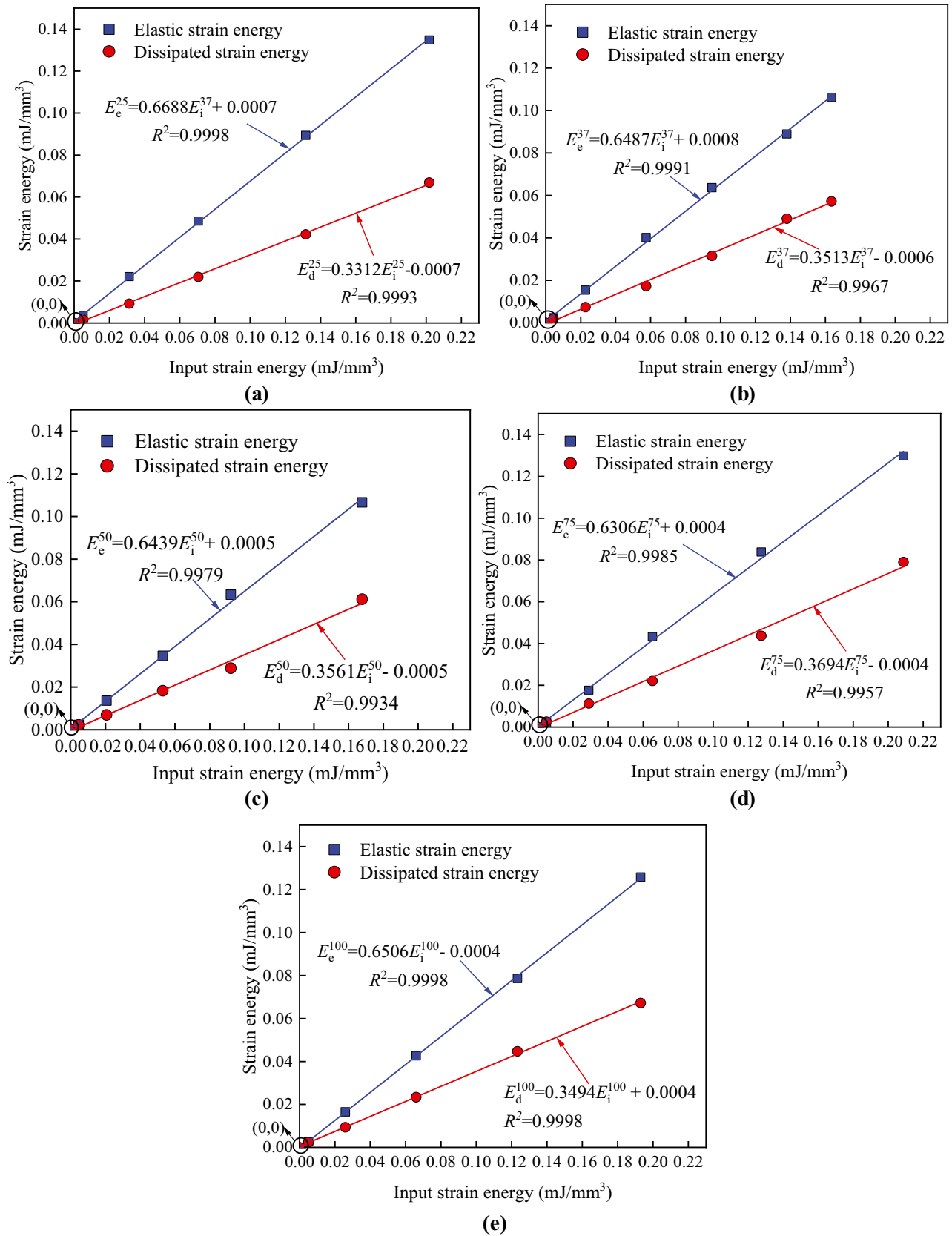


Fig. 8 LES law and LED law of red sandstone with different sizes

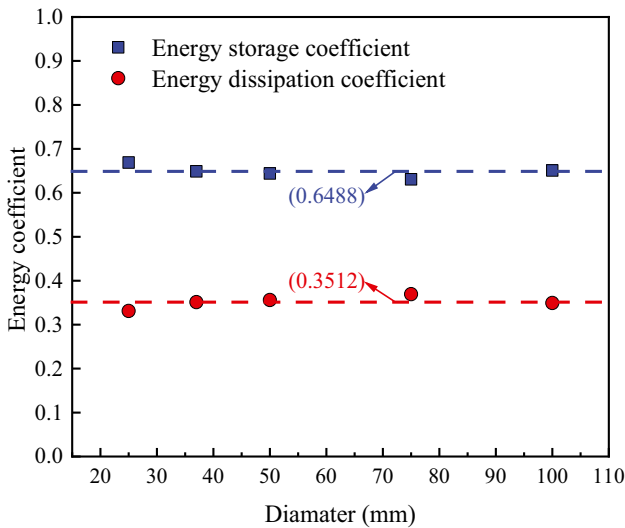


Fig. 9 The ESC and EDC of different specimen sizes

To obtain a general law which describes a relationship between the peak strength and diameter, Fig. 11a shows the peak strength in this study and previous research (i.e., this work and previous studies by Nishimatsu et al. 1969, Hoskins and Horino 1969, Hawkins 1998, Thuro et al. 2001, Pells 2004, Darlington et al. 2011, Masoumi et al. 2016, Komurlu 2018, Walton 2018, Faramarzi and Rezaee 2018, Rong et al. 2018, and Darbor et al. 2019). Due to the reason that the peak strength of various rock types was distinctly different, data were scattered and accurate law was hardly to be observed. Therefore, the peak strength was normalized according to the approach proposed by Hoek and Brown (1980). In Fig. 11b, normalized peak strength equalled peak strength value divided by the peak strength of 50-mm diameter specimen. The formula can be shown as follows:

$$\sigma_{cn} = \frac{\sigma_c^D}{\sigma_c^{50}} \tag{7}$$

where σ_{cn} is normalized peak strength of specimens and σ_c^D is the peak strength of “D” diameter specimens.

Notably, some studies did not include results of $D = 50$ -mm specimens and σ_c^{50} would be replaced by the peak strength of specimens whose diameter was close to 50 mm. Figure 11b reveals that the peak strength increases at first and then decreases slightly with specimen diameters. Specimens whose diameter was ranged from 40 to 60 mm usually had the largest peak strength. Because of the dispersion among peak strength of rock samples, the result in this study was not fully consistent to this general law. Therefore, this conclusion just reflects the general law for the size effect on peak strength, and additional analysis is also needed for specific types of rock.

Size-independent effect on ESC

In the “Linear energy storage and dissipation laws of red sandstone with different sizes” section, it was found that ESC and EDC were not sensitive to specimen sizes by comparing ESC and EDC of specimens of different diameters. However, whether ESC could be considered as an essential property measuring the energy storage capacity of rocks, the variation degree of each parameter under different sizes needed to be compared. As we all known, the P-wave velocity and density were inherent properties whose values were only relevant to rock types, internal components, and structure. On the contrary, mechanical properties such as the peak strength, peak strain, and elastic modulus varied with external loading conditions (e.g., loading rates). In this paper, the coefficient of variation (CoV) was used to evaluate the variation degree of each parameter at different size. The CoV can be defined as follows:

$$\text{CoV} = \frac{\beta}{\mu} \times 100\% \tag{8}$$

where β represents the standard deviation and μ denotes the average value.

CoV values of ESC and other five common parameters were shown in Fig. 12. CoV values of density, ESC, P-wave velocity, peak strain, elastic modulus, and peak strength were 1.30%, 1.89%, 2.37%, 7.7%, 11.33%, and 12.21%, respectively. CoV of the ESC was smaller than that of mechanical properties (peak strain, elastic modulus, and peak strength). Meanwhile, CoV of the ESC was among the range of CoV values of inherent properties (density and P-wave velocity). Hence, ESC reflecting the energy storage capacity of rocks could be considered as an essential property, which did not vary with external loading conditions.

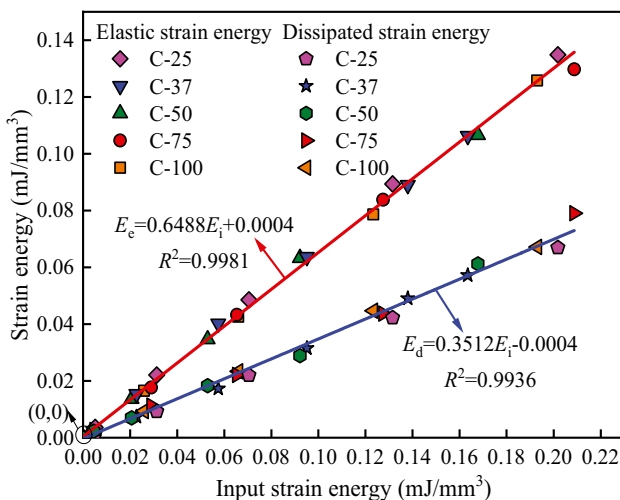


Fig. 10 Unified LES law and unified LED law of specimens with different sizes

Table 2 Summary of the size effect on the peak strength

Specimen type	<i>D</i> (mm)	Conclusions	References
Saajome Andesite	24–70	σ_c increased first and decrease subsequently with the increasing <i>D</i>	Nishimatsu et al. (1969)
Longmont sandstone	25–100	σ_c increased first and keep constant subsequently with the increasing <i>D</i>	Hoskins and Horino (1969)
Hollington Sdst			
Burrington Oolite			
Bath Stone			
Pennant Sdst	12.5–150	σ_c increased first and decrease subsequently with the increasing <i>D</i> . σ_c had the maximum value when <i>D</i> = 38 mm or 54 mm	Hawkins (1998)
Purbeck Lst			
Clifton Down Lst			
Pilton Sdst			
Granite	51–112		
Limestone	45–79	There was no obvious law between <i>D</i> and σ_c	Thuro et al. (2001)
Hawkesbury sandstone	18–144	σ_c slightly increased with the increasing <i>D</i>	Pells (2004)
Concrete mortar	63.5–150	σ_c decreased with the increasing <i>D</i>	Darlington et al. (2011)
Sandstone	19–146	σ_c increased first and then slightly decreased and converged to a constant value with the increasing <i>D</i>	Masoumi et al. (2016)
Akarsen ore			
Siltstone	32–52	σ_c decreased with the increasing <i>D</i>	Komurlu (2018)
Tuff			
Limestone			
Concrete	56–94	σ_c slightly increased with the increasing <i>D</i>	Darbor et al. (2019)
Granite	43–75	σ_c decreased with the increasing <i>D</i>	Walton (2018)
Concrete	56–94	σ_c increased first and decrease subsequently with the increasing <i>D</i>	Faramarzi and Rezaee (2018)
Fine-grained marble	25–100	σ_c decreased with the increasing <i>D</i>	Rong et al. (2018)
Concrete	56–94	σ_c slightly increased with the <i>D</i>	Darbor et al. (2019)
Red sandstone	25–100	σ_c increased for specimens with <i>D</i> = 37–100 mm	This study

where σ_c is the peak strength, *D* is the diameter of specimens, and the length-to-diameter ratio (*L/D*) of all specimens shown above is 2:1

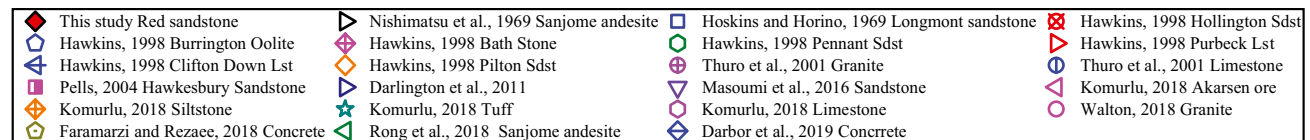
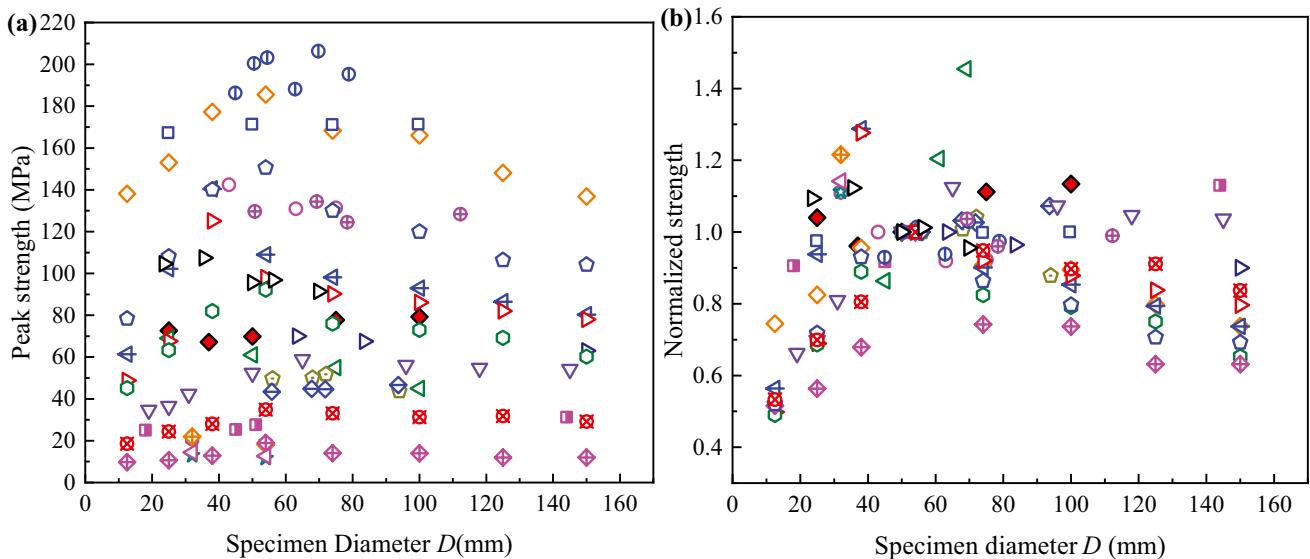


Fig. 11 Relationships between specimen diameter and: **a** peak strength and **b** normalized strength (data from this study and Nishimatsu et al. 1969, Hoskins and Horino 1969, Hawkins 1998, Thuro et al. 2001, Pells 2004, Darlington et al. 2011, Masoumi et al. 2016, Komurlu 2018, Walton 2018, Faramarzi and Rezaee 2018, and Rong et al. 2018, Darbor et al. 2019)

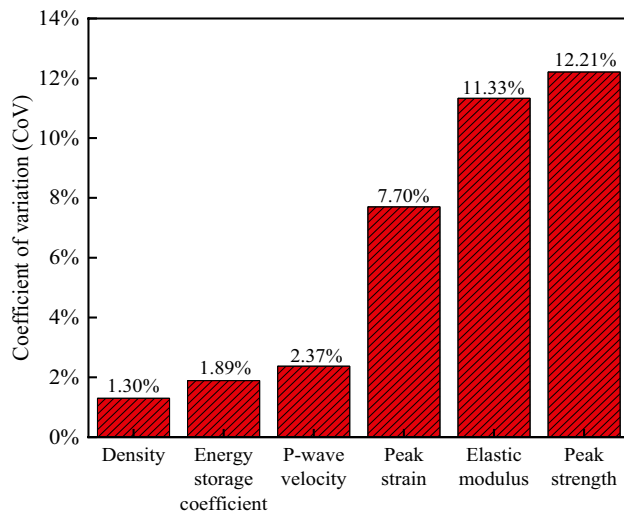


Fig. 12 Coefficients of variation of the ESC and other common parameters

Conclusions

In this study, several groups of UC and SCLUC tests were performed on red sandstone specimens of constant L/D and five different diameters using INSTRON 1346 test system. According to experimental results, effects of specimen size on mechanical properties and failure modes were analyzed. Furthermore, size effects on energy distribution and evolution laws of red sandstone were investigated. The relevant conclusions are as follows:

1. When specimen diameters increased, the concavity of stress–strain curves slightly decreased and the elastic modulus increased. Peak strength increased when D increased from 37 to 100 mm. Peak strain of specimens of $D = 25$ mm was obviously larger than that of other diameters.
2. The failure mode of red sandstone specimens of various diameters was axial splitting failure. The rock failure degree and amounts of rock fragments increased with specimen size. According to analytical results of standard specimens ($D \times L = 50 \text{ mm} \times 100 \text{ mm}$), red sandstone had a low rockburst proneness.
3. The input strain energy (ISE), elastic strain energy (ESE), and dissipation strain energy (DSE) nonlinearly increased with the actual unloading stress level. Unified nonlinear relationships were obtained for specimens whose diameter was from 25 to 100 mm. When the actual unloading stress level increased, ISE had the largest growth rate and DSE had the smallest one.
4. The ESE and DSE linearly increased with the ISE regardless of specimen sizes, i.e., the linear energy storage and dissipation laws also existed for specimens with

non-standard sizes. The energy storage coefficient and energy dissipation coefficient were not dependent on specimen sizes. Furthermore, the energy storage coefficient was an essential property of rock materials which reflected the energy storage capacity of rock materials.

Funding This work was supported by the National Natural Science Foundation of China (Grant No. 42077244, 41877272) and the Fundamental Research Funds for the Central Universities (Grant No. 2242022k30054).

Declarations

Conflict of interest We would like to declare that the work described is original research that has not been published previously and is not under consideration for publication elsewhere, in whole or in part. We declare that we do not have any commercial or associative interest that represents a conflict of interest in connection with the work submitted. The manuscript is approved by all authors for publication.

References

- Bazant ZP (1984) Size effect in blunt fracture: concrete, rock, metal. *J Eng Mech* 110(4):518–535. [https://doi.org/10.1061/\(asce\)0733-9399\(1984\)110:4\(518\)](https://doi.org/10.1061/(asce)0733-9399(1984)110:4(518))
- Carpinteri A, Chiaia B, Ferro G (1995) Size effects on nominal tensile strength of concrete structures: multifractality of material ligaments and dimensional transition from order to disorder. *Mater Struct* 28(180):311–317. <https://doi.org/10.1007/bf02473145>
- Çelik SB (2017) The effect of cubic specimen size on uniaxial compressive strength of carbonate rocks from Western Turkey. *Arab J Geosci* 10(19):426. <https://doi.org/10.1007/s12517-017-3218-3>
- Darbor M, Faramarzi L, Sharifzadeh M (2019) Size-dependent compressive strength properties of hard rocks and rock-like cementitious brittle materials. *Geo Eng* 22(4):179–192. <https://doi.org/10.1080/12269328.2018.1431961>
- Darlington WJ, Ranjith PG, Choi SK (2011) The effect of specimen size on strength and other properties in laboratory testing of rock and rock-like cementitious brittle materials. *Rock Mech Rock Eng* 44(5):513–529. <https://doi.org/10.1007/s00603-011-0161-6>
- Faramarzi L, Rezaee H (2018) Testing the effects of sample and grain sizes on mechanical properties of concrete. *J Mater Civil Eng* 30(5):04018065. [https://doi.org/10.1061/\(ASCE\)MT.1943-5533.0002249](https://doi.org/10.1061/(ASCE)MT.1943-5533.0002249)
- Gong FQ, Luo S, Jiang Q, Xu L (2022) Theoretical verification of the rationality of strain energy storage index as rockburst criterion based on linear energy storage law. *J Rock Mech Geotech Eng.* <https://doi.org/10.1016/j.jrmge.2021.12.015>
- Gong FQ, Wang YL, Luo S (2020) Rockburst proneness criteria for rock materials: review and new insights. *J Cent South Univ* 27(10):2793–2821. <https://doi.org/10.1007/s11771-020-4511-y>
- Gong FQ, Wang YL, Wang ZG, Pan JF, Luo S (2021a) A new criterion of coal burst proneness based on the residual elastic energy index. *Int J Min Sci Technol* 31(4):553–563. <https://doi.org/10.1016/j.ijmst.2021.04.001>
- Gong FQ, Yan JY, Li XB (2018) A new criterion of rock burst proneness based on the linear energy storage law and the residual elastic energy index. *Chin J Rock Mech Eng* 37(9):1993–2014. <https://doi.org/10.13722/j.cnki.jrme.2018.0232>

- Gong FQ, Yan JY, Luo S, Li XB (2019) Investigation on the linear energy storage and dissipation laws of rock materials under uniaxial compression. *Rock Mech Rock Eng* 52(11):4237–4255. <https://doi.org/10.1007/s00603-019-01842-4>
- Gong FQ, Zhang PL, Luo S, Li JC, Huang D (2021b) Theoretical damage characterisation and damage evolution process of intact rocks based on linear energy dissipation law under uniaxial compression. *Int J Rock Mech Min Sci* 146:104858. <https://doi.org/10.1016/j.ijrmm.2021.104858>
- Guo ZH, Luo RY, Li TY, Zou GQ (2017) Influence of size effect on acoustic emission characteristics of rock under uniaxial compression. *AIP Conf Proc* 1890(1):030008. <https://doi.org/10.1063/1.5005196>
- Hawkins AB (1998) Aspects of rock strength. *Bull Eng Geol Env* 57(1):17–30. <https://doi.org/10.1007/s100640050017>
- Hoek E, Brown ET (1980) *Underground excavations in rock*. Inst Min Metall, London, p 156
- Hoskins JR, Horino FG (1969) Influence of spherical head size and specimen diameters on the uniaxial compressive strength of rocks, vol 7234. US Department of the Interior, Bureau of Mines, Report of Investigations, Washington, DC, pp 1–16
- John M (1972) The influence of length to diameter ratio on rock properties in uniaxial compression; a contribution to standardisation in rock mechanics testing. Rep S Afr CSIR No ME1083/5
- Kasyap SS, He H, Senetakis K (2022) 3D DEM analysis of analogue proppant–fractured rock system interaction. *Bull Eng Geol Environ* 81(1):31. <https://doi.org/10.1007/s10064-021-02500-2>
- Kasyap SS, Senetakis K (2022) Small-scale size effects on the shearing behavior and sliding stiffness reduction-displacement curves of rock-plastic gouge simulant under low normal stresses. *J Struct Geol* 157:104553. <https://doi.org/10.1016/j.jsg.2022.104553>
- Khoramshad H, Akbaridoost J, Ayatollahi MR (2014) Size effects on parameters of cohesive zone model in mode I fracture of limestone. *Int J Damage Mech* 23(4):588–605. <https://doi.org/10.1177/1056789513504319>
- Kidybinski A (1981) Bursting liability indices of coal. *Int J Rock Mech Min Sci* 18(4):295–304. [https://doi.org/10.1016/0148-9062\(81\)91194-3](https://doi.org/10.1016/0148-9062(81)91194-3)
- Komurlu E (2018) Loading rate conditions and specimen size effect on strength and deformability of rock materials under uniaxial compression. *Int J Geo-Eng* 9(1):17. <https://doi.org/10.1186/s40703-018-0085-z>
- Lei WS, Qian G, Yu ZS, Berto F (2019) Statistical size scaling of compressive strength of quasi-brittle materials incorporating specimen length-to-diameter ratio effect. *Theor Appl Fract Mech* 104:102345. <https://doi.org/10.1016/j.tafmec.2019.102345>
- Li KH, Yin ZY, Han DY, Fan X, Cao RH, Lin H (2021) Size effect and anisotropy in a transversely isotropic rock under compressive conditions. *Rock Mech Rock Eng* 54(9):4639–4662. <https://doi.org/10.1007/s00603-021-02558-0>
- Li P, Cai MF (2021) Energy evolution mechanism and failure criteria of jointed surrounding rock under uniaxial compression. *J Cent South Univ* 28(6):1857–1874. <https://doi.org/10.1007/s11771-021-4735-5>
- Liang CY, Li X, Zhang H, Li SD, He JM, Ma CF (2013) Research on size effect of uniaxial compression properties of granite under medium and low strain rates. *Chin J Rock Mech Eng* 32(3):528–536
- Liang CY, Zhang QB, Li X, Xin P (2016) The effect of specimen shape and strain rate on uniaxial compressive behavior of rock material. *Bull Eng Geol Environ* 75(4):1669–1681. <https://doi.org/10.1007/s10064-015-0811-0>
- Liu BC, Zhang JS, Du QZ, Tu JF (1998) A study of size effect for compression strength of rock. *Chin J Rock Mech Eng* 17(6):611–614
- Masoumi H, Saydam S, Hagan PC (2016) Unified size-effect law for intact rock. *Int J Geomech* 16(2):04015054. [https://doi.org/10.1061/\(ASCE\)GM.1943-5622.0000543](https://doi.org/10.1061/(ASCE)GM.1943-5622.0000543)
- Meng QB, Zhang MW, Han LJ, Pu H, Li H (2016) Effects of size and strain rate on the mechanical behaviors of rock specimens under uniaxial compression. *Arab J Geosci* 9(8):527. <https://doi.org/10.1007/s12517-016-2559-7>
- Nishimatsu Y, Yamaguchi U, Motosugi K, Morita M (1969) The size effect and experimental error of the strength of rocks. *J Soc Mater Sci Jpn* 18(194):1019–1025. <https://doi.org/10.2472/jsms.18.1019>
- Pells PJN (2004) On the absence of size effects for substance strength of Hawkesbury sandstone. *Aust Geomech* 39(1):79–83
- Perie PJ, Monteiro P (1991) Determination of fracture mechanism by microscopic observation of cracks. *Int J Rock Mech Min Sci Geomech Abstr* 28(1):83–84. [https://doi.org/10.1016/0148-9062\(91\)93236-y](https://doi.org/10.1016/0148-9062(91)93236-y)
- Rong G, Peng J, Yao MD, Jiang QH, Wong LNY (2018) Effects of specimen size and thermal-damage on physical and mechanical behavior of a fine-grained marble. *Eng Geol* 232:46–55. <https://doi.org/10.1016/j.enggeo.2017.11.011>
- Song HH, Jiang YD, Elsworth D, Zhao YX, Wang JH, Liu B (2018) Scale effects and strength anisotropy in coal. *Int J Coal Geol* 195:37–46. <https://doi.org/10.1016/j.coal.2018.05.006>
- Su HJ, Jing HW, Mao XB, Zhao HH, Yin Q, Wang C (2015) Size effect of sandstone after high temperature under uniaxial compression. *J Cent South Univ* 22(5):1901–1908. <https://doi.org/10.1007/s11771-015-2709-1>
- Su YQ, Gong FQ, Luo S, Liu ZX (2021) Experimental study on energy storage and dissipation characteristics of granite under two-dimensional compression with constant confining pressure. *J Cent South Univ* 28(3):848–865. <https://doi.org/10.1007/s11771-021-4649-2>
- Thuro K, Plinninger RJ, Schutz SZS (2001) Scale effects in rock strength properties. Part 1: Unconfined compressive test and Brazilian test. Proceedings of ISRM regional symposium EUROCK 2001: rock mechanics—a challenge for society. A.A. Balkema, Espoo, pp 169–174
- Walton G (2018) Scale Effects observed in compression testing of stanstead granite including post-peak strength and dilatancy. *Geotech Geol Eng* 36(2):1091–1111. <https://doi.org/10.1007/s10706-017-0377-7>
- Wu FQ, Qiao L, Guan SG, Zhang QT, Wang ZY, Wu J (2021) Uniaxial compression test study on size effect of small size rock samples. *Chin J Rock Mech Eng* 40(5):865–873. <https://doi.org/10.13722/j.cnki.jrme.2020.0555>
- Wu SC (2021) *Rock Mechanics*. Beijing, China
- Xie HP, Ju Y, Li LY (2005) Criteria for strength and structural failure of rocks based on energy dissipation and energy release principles. *Chin J Rock Mech Eng* 24(17):3003–3010. <https://doi.org/10.3321/j.issn:1000-6915.2005.17.001>
- Yang SQ, Su CD, Xu WY (2005) Experimental and theoretical study on size effect of rock materials. *Eng Mech* 22(4):112–118. <https://doi.org/10.3969/j.issn.1000-4750.2005.04.022>
- You MQ, Zou YF (2000) Discussion on rock heterogeneity and strength size effect. *Chin J Rock Mech Eng* 19(3):391–395. <https://doi.org/10.3321/j.issn:1000-6915.2000.03.031>
- Zhao F, He MC (2017) Size effects on granite behavior under unloading rockburst test. *Bull Eng Geol Environ* 76:1183–1197. <https://doi.org/10.1007/s10064-016-0903-5>
- Zhao GM, Liu ZX, Meng XR, Zhang RF, Kao SM, Qi MJ (2022) Energy accumulation and dissipation test and analysis method of height-diameter ratio sandstone. *J Chin Coal Soc* 47(3):1110–1121. <https://doi.org/10.13225/j.cnki.jccs.xr21.1606>

Springer Nature or its licensor holds exclusive rights to this article under a publishing agreement with the author(s) or other rightsholder(s); author self-archiving of the accepted manuscript version of this article is solely governed by the terms of such publishing agreement and applicable law.